Polymer Testing
October 2014, Volume 39, Pages 36-44
http://dx.doi.org/10.1016/j.polymertesting.2014.07.009

Novel mechanical characterization method for deep sea buoyancy material under hydrostatic pressure

Maelenn Le Gall[a,] *, Dominique Choqueuse[a], Pierre-Yves Le Gac[a], Peter Davies[a], Dominique Perreux[b]

[a] IFREMER, Centre de Bretagne, Marine Structures Group, CS 10070, 29280 Plouzané, France
[b] Université de Franche Comté, UMR6174 Institut FEMTO-ST, 25000 Besançon, France

*: Corresponding author : Maelenn Le Gall, email address : maelenn.le.gall@ifremer.fr

Abstract:

Syntactic foams, used in submersibles and in pipelines for deep sea oil wells, must be resistant to the severe conditions of the deep sea environment. As these foams will be in service for at least 20 years, their qualification testing is crucial. However, their mechanical characterization under real conditions of use is a challenge. In deep sea, the main loading is hydrostatic compression, however there is no standard procedure for testing material under pure hydrostatic pressure. The aim of this paper is to present a new characterization technique based on buoyancy loss measurement under hydrostatic pressure. To validate the method, two different syntactic foams (one brittle and one ductile) have been tested. Their behaviours under hydrostatic pressure have been followed by the proposed technique. The results from this innovative characterization technique have been compared to those of traditional uniaxial compression tests performed on the same materials.

Keywords: Hydrostatic compression ; Syntactic foam ; Deep sea ; Mechanical characterization

1. Introduction

The oceans represent more than 70% of the surface of the earth and most of them remain unexplored. This is due both to technological challenges as well as economic reasons. However, with the increase of the oil barrel price, deep sea oil wells become economically viable. This leads to the development of new technologies and materials for exploration and exploitation purposes. As an example, syntactic foams have been developed in the 1960's for buoyancy in deep sea exploration applications [1] and [2]. They are one of the main components of the Ifremer manned submersible, Nautile, which can go down to 6000 m, shown in Fig. 1.

Syntactic foams are made of fillers embedded in a polymeric matrix. The fillers are often hollow glass spheres in the micrometer range. Glass microspheres have been described in detail by Ruckebush [3]. Depending on the nature of the components, the syntactic foams' functional properties are light weight, high hydrostatic strength and long term integrity in a deep sea environment. Syntactic foams are also used for their thermal insulation properties in deep sea oil exploitation [4]. Indeed, in deep sea, oil has to be kept above 40°C in order to avoid the formation of wax and hydrates, and to maintain the flow. Syntactic foams are used in various other applications. Bibin has recently provided an exhaustive review of their applications and uses [5]. To be used in harsh environment, the materials have to be qualified in conditions simulating the conditions of use. In deep sea, the structures are subjected to high mechanical stresses. The characterization of the mechanical behaviour of syntactic foam is of primary interest and it has been extensively studied during the last decade. Most of the published studies refer to uniaxial compressive behaviour, e.g; Kim [6], Gupta [7, 8], Karthikeyan [9], Song [10], Tagliava [11], Aureli [12], Poveda [13], Porfiri [14]. However, in the case of buoyancy for submarine structures, the loading condition is hydrostatic compression. If the material used is coated or bonded to a surface, it is also subjected to deviatoric stresses. To a first approximation, the behaviour of submarine foam can be evaluated by hydrostatic compression testing. However, as far as the authors are aware, there is no standard equipment for material characterization under purely hydrostatic compression at high pressure. The aim of the present work is to provide a new methodology for the evaluation of the mechanical behaviour of syntactic foams under such loading. For this study, two syntactic foams made with the same glass microspheres are used: glass epoxy syntactic foam (GSEP) and glass syntactic polyurethane (GSPU). The material itself will not be extensively described in this work; these two syntactic foams, both industrially used, have simply been chosen for their differences in behaviour (one ductile and one brittle). In the first

part of this paper, the foams will be studied by a traditional uniaxial compression test method. In the second part, the development of the new characterization technique will be presented and the foams will be characterized. Finally, a comparison between the results from both techniques will be reported.

"Figure 1"

2. Materials

The syntactic foams studied in the present work are designated as GSEP and GSPU. For both materials, the fillers are glass hollow microspheres grade S38 from 3M™. The two foams were made by casting. Their specific gravities are 0.72 and 0.86, respectively. The volume content of microspheres is around 55% for the GSEP and 25% for GSPU.

3. Traditional tests

3.1 Test method

Uniaxial compression tests are frequently used to provide information on the behaviour of the syntactic foams. Standards are available [15, 16], but sample geometry is not strictly defined. Usually, a straight cylinder is preferred, but a specially designed dumbbell geometry presents the advantages of localizing the maximum deformation in the calibrated part of the specimen and limiting the edge effects in the load introduction area. In the present work, these two geometries have been tested. Their descriptions are given in Table 1.

"Table 1"

Tests were performed at 20°C ± 1°C and 50 RH%, with a 200 kN capacity electro-mechanical test frame with a loading rate of 2 mm/min. Samples were equipped with strain gauges, and an axial extensometer was also mounted.

Digital Image Correlation (DIC) was used on some specimens. DIC allows the measurement of the strain field versus applied load from high resolution images. The equipment used was an Aramis 5M system from the GOM Company. The 3D mode was used and the calibration panel was 90*72 mm². For type 1 specimens, the axial line covers the whole length of the sample. For type 2 specimens, the area analyzed covers half of the length. The position 0 corresponds to the central part of both types of samples as shown in Figure 2.

"Figure 2"

3.2 Results of traditional tests

The behaviour of both materials, GSEP and GSPU, under uniaxial compression has been investigated, as shown in Figure 3.

"Figure 3"

The stress-strain curves of GSEP and GSPU show a non linear response for the two geometries. However, the behaviour of the two materials is significantly different. GSEP presents a stress at break up to 98 MPa, which is around 8 times higher than that of GSPU. For GSPU, one can observe that buckling governs the collapse of the specimen. For both materials, a significant difference in behaviour for the 2 types of geometry is also noted. To get a better understanding of this phenomenon and to define the most pertinent geometry, a more detailed investigation has been performed by DIC. The results from uniaxial compression tests, recorded with DIC system, for the two types of geometry of GSEP and GSPU, are reported in Figures 4 and 5, respectively.

"Figure 4"

"Figure 5"

One can observe that, for GSPU and GSEP type 1 samples, the strain distribution is not homogeneous along the length, particularly under high load. A significant barrelling effect is observed, which can also be observed on Figure 6. For type 2 samples, as the measurement region extends to the wider specimen ends, only a calibrated central area was analyzed. In this area, the strain distribution is homogeneous along the line for the two materials, suggesting that this is an improved specimen compared to the standard cylindrical shape. GSEP and GSPU representing a large range of materials, one can conclude that the dumbbell geometry, called type 2 in the present work, is the more suitable for uniaxial compression tests.

"Figure 6"

For repeatability purposes, several samples (2 GSPU and 3 GSEP), with type 2 geometry, have been tested under uniaxial compression. Results are presented in Table 2. Young's moduli, Poisson's coefficients and stresses at break were obtained experimentally, while bulk moduli values were calculated from experimental data. However, even if those results are relevant for material characterization, one can question the pertinence of uniaxial compression tests to understand the behaviour of syntactic foams under hydrostatic pressure.

"Table 2"

4. Development of a new test method

4.1 Confined pressure equipment

The reproduction of hydrostatic pressure conditions experienced by the material in deep water remains a real challenge. Some standards [17, 18] have addressed this topic in the past but they have been withdrawn. A confined compression cylinder test has been developed; although not purely hydrostatic, it is expected to be more hydrostatic than a standard uniaxial compression test. By the use of a confinement ring, the hydrostatic loading is coupled with

uniaxial compression loading. A testing procedure dedicated to syntactic foam using this confined pressure test has been proposed for the oil and gas industry [19]. One of the main challenges of this technique is the evaluation of the loading conditions, which are strongly affected by the accuracy of the machining of the samples. Adrien et al. found that the damage developed was dependent on the stiffness of the foam [20]. They also questioned the homogeneity of the loading state and the possibility of inducing damage in a preferred direction with respect to the applied piston displacement. For these reasons, this technique, while offering an intermediate test between uniaxial and full hydrostatic loading, will not be evaluated in this study.

4.2 Hydrostatic pressure equipment

Recently, some publications addressed the volume variation of material versus pressure, and the behaviour of the material under hydrostatic compression [21-24]. However, those studies have been performed at relatively low pressure (<10MPa). In our study, the requirements are the conditions experienced by the foams in deep sea environment: pressure up to 100 MPa and temperature from 2°C to 160°C. Tests at temperatures up to 160°C are needed to qualify the foam used as passive insulation in deep sea pipelines.

In thermal insulation applications for offshore, external seawater is around 4°C while oil inside the pipe should be kept above 40°C to avoid hydrate formation. The foams are subjected to high thermal gradient and, consequently, they have to be qualified at high temperature. In specifying the accuracy of the novel characterization method, the volume variation should be measured continuously and the sensitivity of volume change measurement should be better than 1%.

4.2.1 *Hyperbaric compression test based on piston displacement*

The first equipment, developed in an attempt to improve upon the existing tests, was an hyperbaric compression test based on piston displacement. The principle was to record the displacement of a piston which generates an increase of pressure in a hyperbaric tank, as shown in Figure 7. The advantage of this approach is the simplicity of the tank which can be mounted on a standard test machine.

"Figure 7"

A 43 cm^3 GSPU sample has been tested up to 60 MPa with that device. The hyperbaric tank was placed on a 200 kN test machine. The test has been performed at room temperature and with a loading rate of 2mm/min. The results presented as the volume change of the sample as a function of the pressure change are reported in Figure 8. The evolution of the water alone, tested under the same conditions, is used as a reference. One can observe that up to 20 MPa the material behaviour follows that of the water. Around 30 MPa an inflexion point is observed. This corresponds to the damage of the foam.

"Figure 8"

To conclude on that device, it allows the behaviour of the foam to be followed as a function of the hydrostatic pressure. However, it presents several limitations; air can pollute the response and make the analysis difficult, the sample dimensions are restricted, it is difficult to heat up the system and the components are subjected to thermal dilatation at temperatures higher than 90°C.

4.2.2 *Hyperbaric compression test based on buoyancy measurement*

In order to overcome the limitations of that first design, a second improved device was developed based on buoyancy measurement. The principle is to apply hydrostatic pressure to a specimen through a loading fluid and to follow its buoyancy throughout the duration of the

test. The buoyancy of the sample is directly measured by a weighing device. With Archimedes' principle, it is possible to evaluate the volume change of the material as a function of the pressure (1):

$$F = \rho_{water} V_{material} g - \rho_{material} V_{0material} g \qquad (1)$$

where F is the buoyancy force of the sample (N), ρ_{water} is the density of the water, $\rho_{material}$ is the density of the material, $V_{material}$ is the volume of the material (m^3), $V_{0material}$ is the initial volume of the material (m^3) and g is the gravitational acceleration ($m.s^2$).

The changes of seawater properties have to be taken into account in the system. Those are defined by the state equation of seawater from the international Thermodynamic Equation Of Seawater-2010 (TEOS10). The relation between pressure and depth is defined from the method developed by Saunders & Fofonoff [25]. An approximate correspondence is also provided in the oceanographic equipment qualification standard [26]. The aim of the present paper is to present a new characterization technique, therefore we will not consider here the water uptake nor the influence of the nature of the water.

An in-house control system of the pressure has been developed which allows both quasi static and creep tests to be performed by maintaining constant pressure over a fixed time. The equipment developed can be seen in Figures 9 and 10.

"Figure 9"

"Figure 10"

4.2.2.1 Experimental

The system is equipped with a hyperbaric weighing device from Sixaxes™, specification 5N-150°C. This type of weighing device, designed to be temperature and

pressure compensated, can resist up to 1000 bars. The pressure sensor is a Pt 100. The heating device is an articulated ceramic band heater 3 Vulcanic™ type 4030 and the heating controller is a thermostat control unit 32060-13 from Vulcanic™. The data logger is an AB22 model from HBM™. All the tests have been performed with a pressure ramp of 10 bar/min.

4.2.2.2 Results and discussion

GSPU and GSEP 1 dm^3 samples were tested up to 60 MPa. For both materials, the results are presented as loss of volume and loss of buoyancy as a function of the hydrostatic pressure, as shown in Figure 11. One can observe a significant difference between the two materials for both the loss of volume and the loss of buoyancy. Concerning the loss of buoyancy, one can observe a gain of buoyancy for GSEP up to 30 MPa, whereas the GSPU sample presents a loss of buoyancy even at low pressure. This is explained by the bulk modulus of the materials. GSEP has a bulk modulus higher than that of the water (2.2 GPa at room temperature), which explains the increase of the buoyancy of the material with pressure increase up to 30 MPa. GSPU has a bulk modulus lower than that of water. When the water density changes are accounted for, both materials present a linear decrease of the volume as a function of the pressure. Consequently, it is more representative of the material behaviour. All the subsequent results will be presented with volume variation plotted as a function of the hydrostatic pressure.

"Figure 11"

A 1 dm^3 GSPU sample has been tested at room temperature up to 40 MPa. The results are presented in Figure 12. One can observe the non linear behaviour of the volume variation with the increase of pressure. Around 30 MPa, an inflexion point is observed showing the sudden collapse of the material. Due to the non linear behaviour of the material, the bulk modulus has been defined to be the secant modulus at 1% strain. The crush pressure is

defined to be the pressure corresponding to the intersection between the bulk modulus slope and the slope of the plateau.

"Figure 12"

For repeatability purposes, three samples of around 1 dm^3 of GSPU have been tested at room temperature. As can be observed in Figure 12, the results are very similar with a deviation of approximately 5%.

To verify the pertinence of the method, GSPU samples of various sizes have been tested at room temperature up to 40 MPa. The results are shown on Figure 13. One can observe very good correspondence between the samples of various sizes from the same material; no scale effects are observed for those samples in the cubic decimeter range.

"Figure 13"

1 dm^3 GSPU and GSEP samples have been tested at room temperature as shown in Figure 14. One can observe a significant difference between the two materials. Whereas GSPU exhibits non linear behaviour and a plateau at 40 MPa, GSEP material exhibits linear behaviour up to 80 MPa followed by a sudden collapse of the material. The block of material is cracked at this pressure and is no longer buoyant. The bulk modulus and the crush pressure for both materials at 20°C are calculated and presented in Table 3. The behaviour of the materials is qualitatively in agreement with the results obtained with traditional compression tests, GSEP showing brittle behaviour whereas GSPU is ductile.

"Figure 14"

"Table 3"

The new equipment has also been tested at different temperatures, up to 100°C. Figure 15 shows results from hydrostatic compression tests at different temperatures on the GSEP and GSPU materials. One can observe that the crush pressure drops with the increase of the temperature for both materials. For GSEP, there is no significant change in the initial bulk modulus but for GSPU a significant difference is noticed. For GSEP, one can observe an intermediate slope change between the initial slope and the plateau. Further studies will be needed to clarify the reasons for this behaviour.

"Figure 15"

The results obtained with both techniques for the two materials are compared in Table 4. As discussed before, the two materials present very different characteristics. For both materials, the bulk modulus from hydrostatic compression test and the bulk modulus from uniaxial compression test are different. This is due to the difference of load (hydrostatic or uniaxial). It should also be noted that the duration of tests was different: 40 to 60 minutes for hydrostatic compression test compared to approximately 5 minutes for uniaxial compression. Therefore, differences may also be explained by the viscoelastic behaviour of the materials. For GSEP, the stress at break and the crush pressure are of similar orders of magnitude. For GSPU, the stress at break could not be reached. It should also be noted that the damage behaviour of these two types of foam material is quite different. Choqueuse [27] has shown using pressure tests inside a micro-tomograph that, while collapse of microspheres in GSEP results in no volume change, this is not the case for GSPU. For the latter, the collapse of spheres causes a global volume reduction and densification as the matrix fills the broken spheres, but when pressure is released the specimen recovers its initial volume through viscoelastic recovery.

"Table 4"

Both techniques, standard uniaxial compression and hydrostatic compression, do not provide the same data but present advantages. The first technique can be performed on a standard test machine and can be done very quickly. However, with a uniaxial compression test the conditions of use of the syntactic foams are not simulated. Moreover, for material presenting a complex viscoelastic behaviour, such as GSPU, structural buckling of the specimen may appear. The second technique has also shown its potential to characterize different types of foams, GSEP and GSPU being representative of a broad range of materials. With this technique, the foams can be characterized at different temperatures and their behaviour, under conditions simulating the conditions of use, can be studied.

5. Conclusions

The qualification of syntactic foams is crucial. However, their characterization under conditions simulating conditions of use is a challenge. Standard uniaxial compression tests have been performed on GSPU and GSEP materials. Despite geometry optimization of the samples, limitations are observed mainly for ductile materials, such as GSPU, where buckling occurs. A new characterization technique based on buoyancy loss under hydrostatic pressure has been developed. GSEP and GSPU materials have been tested with this equipment. The materials behaviour under hydrostatic pressure has been characterized, with determination of bulk modulus and crush pressure values. However, further investigations need to be performed, particularly on the behaviour of the foams at different temperatures and loading rates. The method proposed here appears promising and provides a characterization of the foam under hydrostatic load. Moreover, this technique allows creep and dynamic tests to be performed. It is now being used to develop a better understanding of material behaviour for underwater applications.

6. Acknowledgement

The authors thank P. Beriet, B. Forest, N. Lacotte, C. Peyronnet, M. Premel-Cabic and L. Riou from Ifremer for their help in performing the tests described here.

7. References

1. G. Fontblanc. Mousses syntactiques : matériaux composites pour grandes profondeur. Doctorat thesis. Bordeaux University. 1986
2. F.A. Shutov. Syntactic polymer foams. Advances in Polymer Science 1986; 73/74:63.
3. J.M. Ruckebusch. Microspheres creuses de verre pour mousses syntactiques. Techniques de l'Ingénieur. 2009
4. U. Okonkwo, F. Uralil, E. Berti, S. Judd In: Proceedings of Deep Offshore Technology, Vittoria, Brazil, 2005
5. J. Bibin, C.P.Reghunadhan Nair. Update on syntactic foams. iSmithers. 2010
6. H.S. Kim, P. Plubrai. Manufacturing and failure mechanisms of syntactic foam under compression. Composites Part A- Applied Science and Manufacturing 2004; 35(9):1009.
7. N. Gupta, E. Woldesenbet, P. Mensah. Compression properties of syntactic foams: effect of cenosphere radius ratio and specimen aspect ratio. Composites Part a-Applied Science and Manufacturing 2004; 35(1):103.
8. N. Gupta, E. Woldesenbet, Kishore. Compressive fracture features of syntactic foams-microscopic examination. Journal of Materials Science 2002; 37(15):3199.
9. C.S. Karthikeyan, S. Sankaran, and Kishore. Elastic behaviour of plain and fibre-reinforced syntactic foams under compression. Materials Letters 2004; 58(6):995.
10. B. Song, W. Chen. Dynamic compressive response and failure behavior of an epoxy syntactic foam. Journal of Composite Materials 2004; 38(11):915.
11. G. Tagliavia, M. Porfiri, N. Gupta. Analysis of particle-to-particle elastic interactions in syntactic foams. Mechanics of Materials 2011; 43(12):952.
12. M. Aureli, M. Porfiri, N. Gupta. Effect of polydispersivity and porosity on the elastic properties of hollow particle filled composites. Mechanics of Materials 2010; 42(7):726.
13. R. Poveda, N. Gupta, M. Porfiri. Poisson's ratio of hollow particle filled composites. Materials Letters 2010; 64(21):2360.
14. M. Porfiri, N. Gupta. Effect of volume fraction and wall thickness on the elastic properties of hollow particle filled composites. Composites Part B-Engineering 2009; 40(2):166.
15. ASTM, ASTM D695 - 10. Standard Test Method for Compressive Properties of Rigid Plastics. 2010
16. ASTM, ASTM D1621 - 10. Standard Test Method for Compressive Properties Of Rigid Cellular Plastics. 2010
17. ASTM D2736-78. Practice for Determination of Hydrostatic Compressive Strength of Syntactic Foam. 1982 (Withdrawn 1984)
18. ASTM D2926-70. Method of Test for Bulk Modulus of Elasticity of Syntactic Foam (Piston-Cylinder Method). 1976 (Withdrawn 1987)

19. ISO/DIS 12736, Petroleum and natural gas industries. Wet thermal insulation coatings for pipelines, flow lines, equipment and subsea structures. 2012

20. J. Adrien, E. Maire, N. Gimenez, V. Sauvant-Moynot. Experimental study of the compression behaviour of syntactic foams by in situ X-ray tomography. Acta Materialia 2007; 55:1667.

21. Y. Kim, S. Kang. Development of experimental method to characterize pressure-dependent yield criteria for polymeric foams. Polymer Testing 2003; 22(2) : 197.

22. P. Viot. Hydrostatic compression on polypropylene foam. International Journal of Impact Engineering 2009; 36(7):975.

23. U.E. Ozturk, G. Anlas. Hydrostatic compression of anisotropic low density polymeric foams under multiple loadings and unloadings. Polymer Testing 2011; 30(7) : 737.

24. Y.M. Moreu, N.J. Mills. Rapid hydrostatic compression of low-density polymeric foams. Polymer Testing 2004; 23(3):313.

25. P.M. Saunders, N.P. Fofonoff. Conversion of Pressure to Depth in Ocean. Deep-Sea Research 1976; 23(1):109.

26. AFNOR, Milieu marin - Instrumentation océanographique - Guide d'essais en environnement. XP X10-800. 1995

27. D. Choqueuse. Experimental study and analysis of the mechanical behaviour of syntactic foams used in deep sea. Doctorat thesis. University of Franche-Comté. 2012 available from http://archimer.ifremer.fr/doc/00114/22573/20263.pdf

8. Figure captions

Figure 1. Ifremer manned submersible Nautile

Figure 2. Compression sample geometry and location of measurement

Figure 3. Uniaxial compression testing of GSEP on the left, and of GSPU on the right

Figure 4. Compression curve and strain distribution on GSEP type 1 and type 2 specimens

Figure 5. Compression curve and strain distribution on GSPU type 1 and type 2 specimens

Figure 6. Barrelling effect on GSPU type 1 sample during uniaxial compression test

Figure 7. Hyperbaric compression test based on piston displacement

Figure8. Hydrostatic compression curve for GSPU at 20°C

Figure 9. Schematic diagram of hydrostatic compression test using immersed balance

Figure 10. Photo of hydrostatic compression test system

Figure 11. Comparison between loss of volume and loss of buoyancy for GSEP, on the right, and GSPU, on the left, materials under hydrostatic compression test

Figure12. Volume variation of 1dm^3 GSPU samples subjected to hydrostatic pressure

Figure 13. Influence of the sample volume on hydrostatic compression test results

Figure 14. Hydrostatic compression test at 20°C

Figure 15. Influence on the temperature for GSEP material, on the left, and GSPU, on the right during hydrostatic compression test

1. Tables

Table 1. Sample geometry for uniaxial compression test

Type	Shape	Diameter (mm)	Length (mm)	Calibrated length (mm)
1	Right cylinder	12.5	25	25
2	Dog bone cylinder	13	65	27

Table 2. Uniaxial compression test at 20°C

	GSEP	GSPU
Young modulus (GPa)	3.34 ± 0.20	0.43 ± 0.04
Poisson's Coefficient	0.34 ± 0.01	0.49 ± 0.04
Stress at break (MPa)	97.8 ± 5.2	11.7 ± 0.9
Bulk modulus (GPa)	3.5 ± 0.3	7.2 ± 1.3

Table 3. Hydrostatic compression test at 20°C

	GSEP	GSPU
Bulk modulus (GPa)	2.62 ± 0.03	1.91 ± 0.02
Crush pressure (MPa)	83.0 ± 1.7	32.4 ± 0.6

Table 4. Results from uniaxial compression test and hydrostatic compression test

		GSEP	GSPU
Bulk modulus (GPa)	Uniaxial compression	3.5 ± 0.3	7.2 ± 1.3
	Hydrostatic compression	2.62 ± 0.03	1.91 ± 0.02
Stress at break (MPa)		97.8 ± 5.2	11.7 ± 0.9
Crush pressure (MPa)		83.0 ± 1.7	32.4 ± 0.6

1. Figures

Figure 1. Ifremer manned submersible Nautile

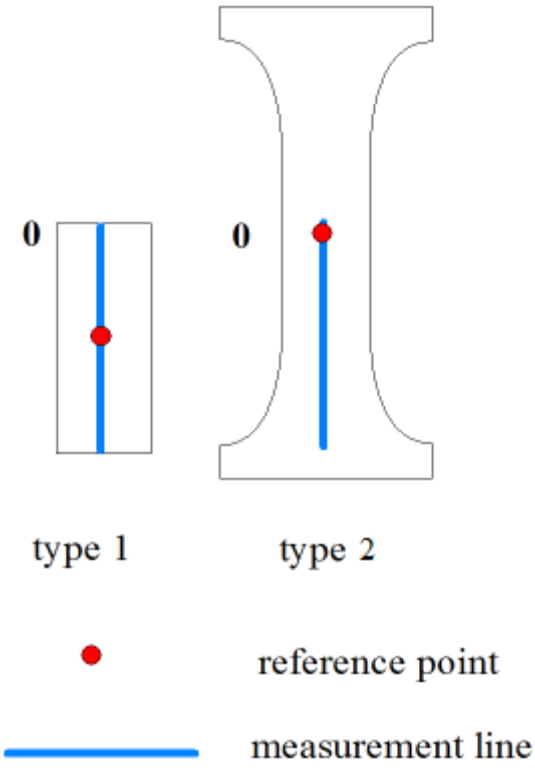

Figure 2. Compression sample geometry and location of measurement

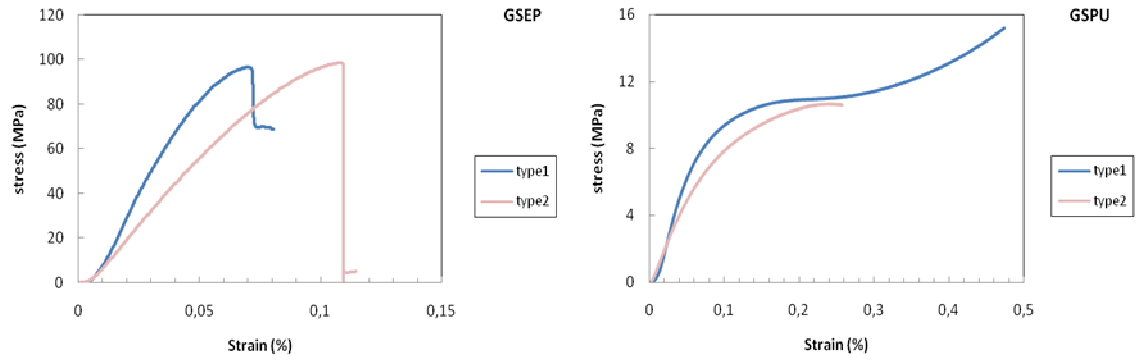

Figure 3. Uniaxial compression testing of GSEP on the left, and of GSPU on the right

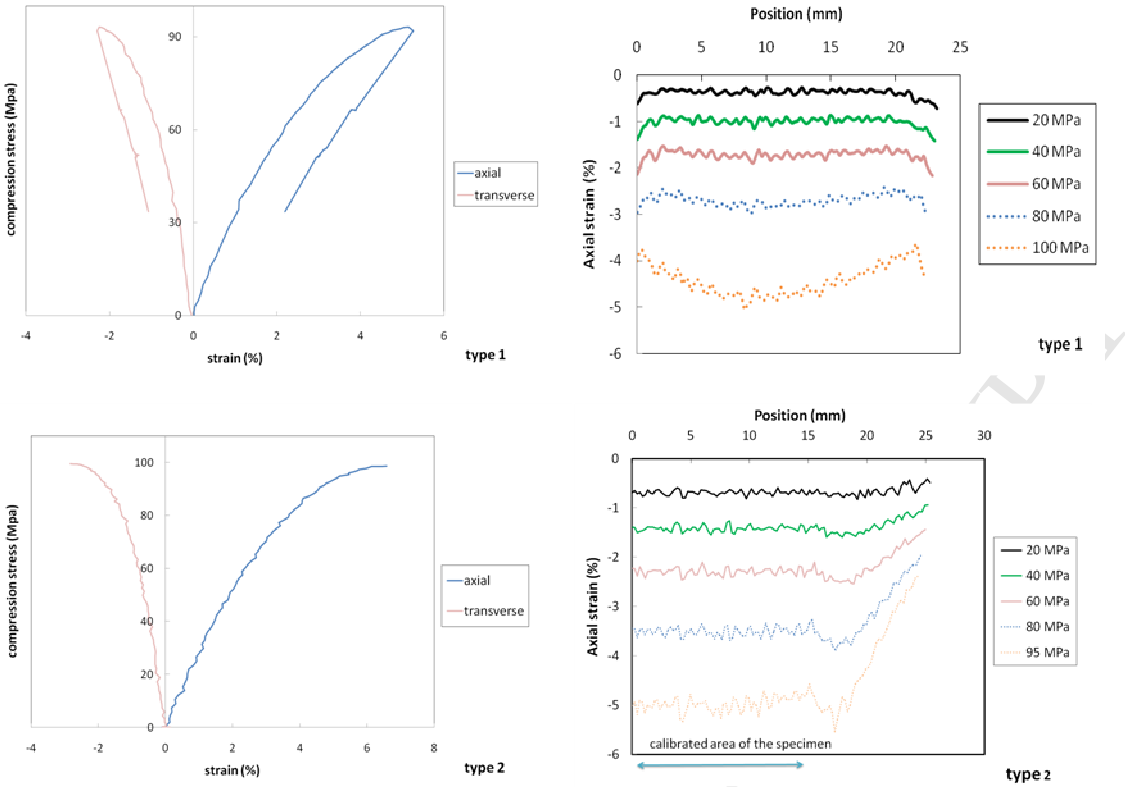

Figure 4. Compression curve and strain distribution on GSEP type 1 and type 2 specimens

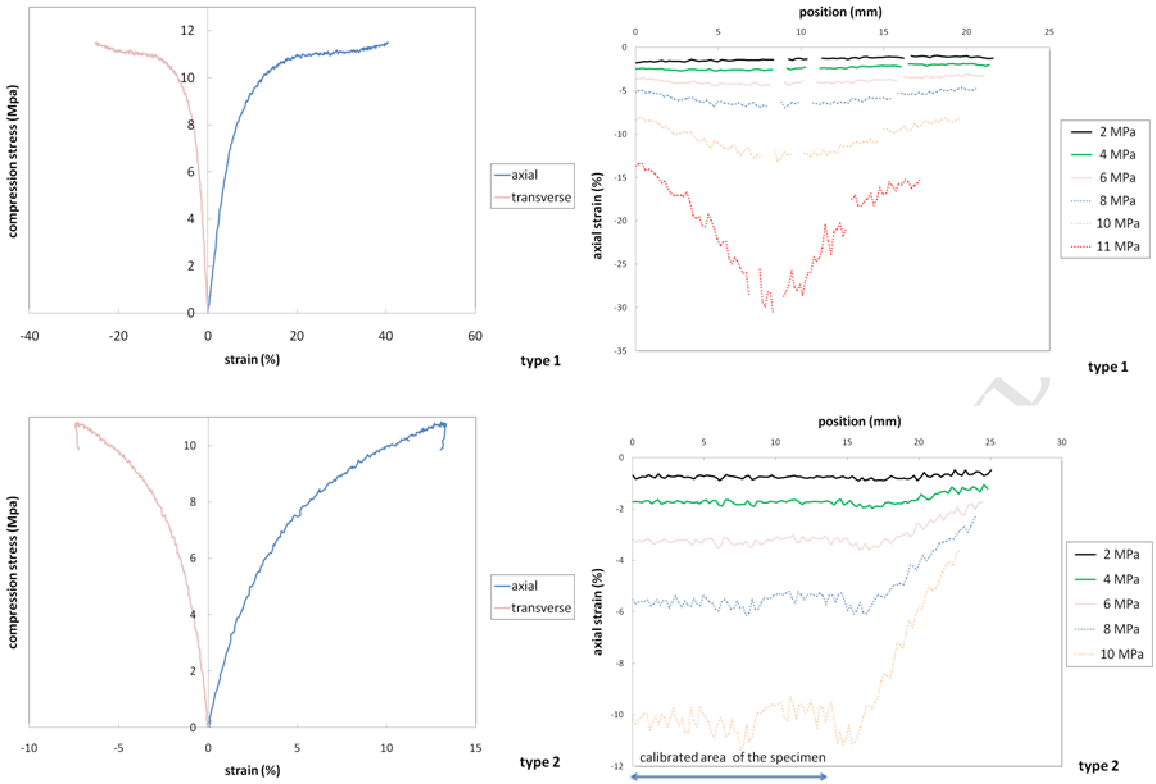

Figure 5. Compression curve and strain distribution on GSPU type 1 and type 2 specimens

Figure 6. Barrelling effect on GSPU type 1 sample during uniaxial compression test

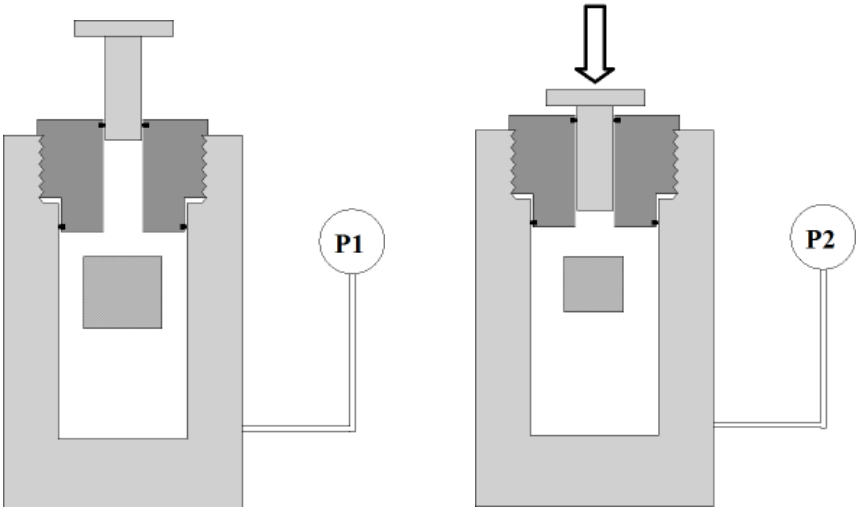

Figure 7. Hyperbaric compression test based on piston displacement

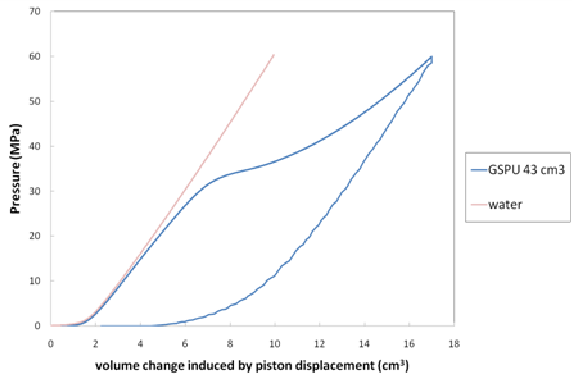

Figure 8. Hydrostatic compression curve for GSPU at 20°C

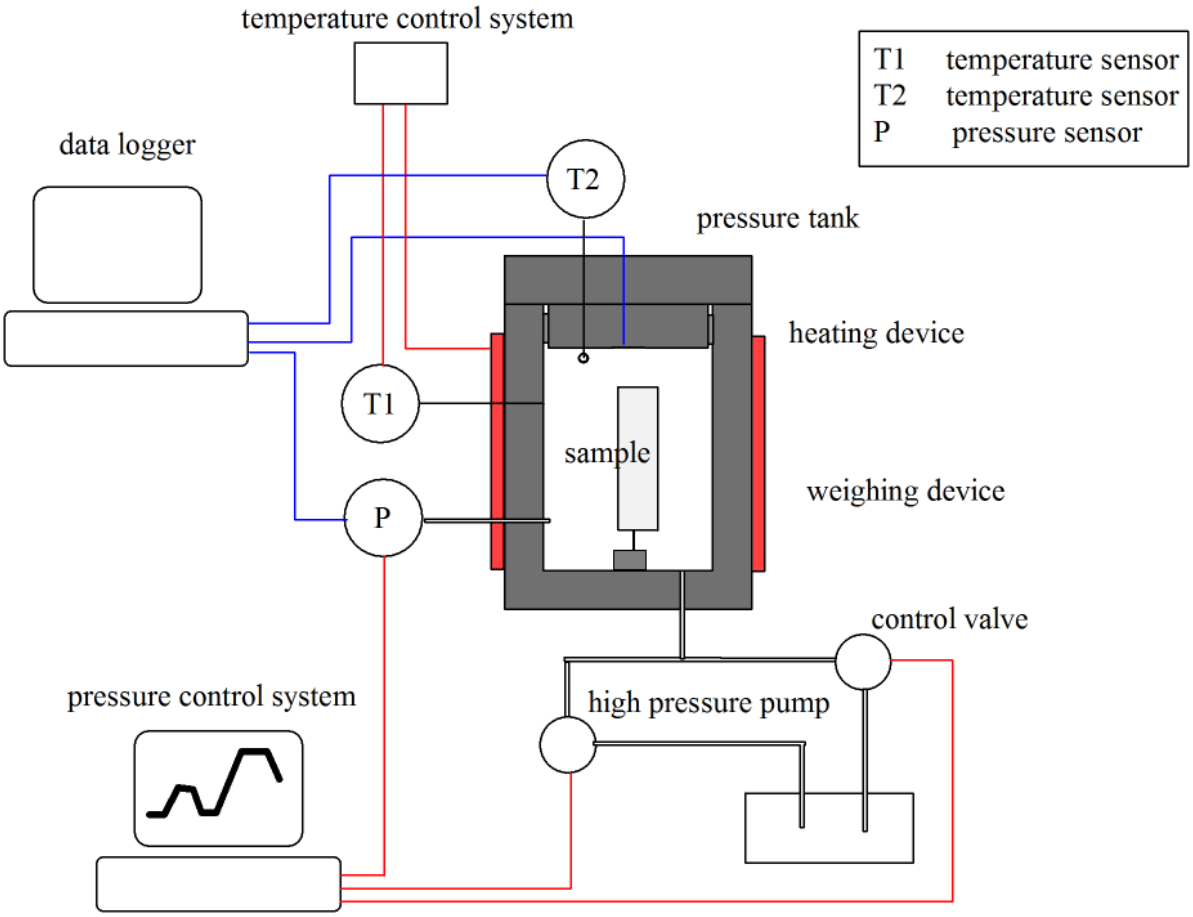

Figure 9. Schematic diagram of hydrostatic compression test using immersed balance

Figure 10. Photo of hydrostatic compression test system, internal diameter 300 mm

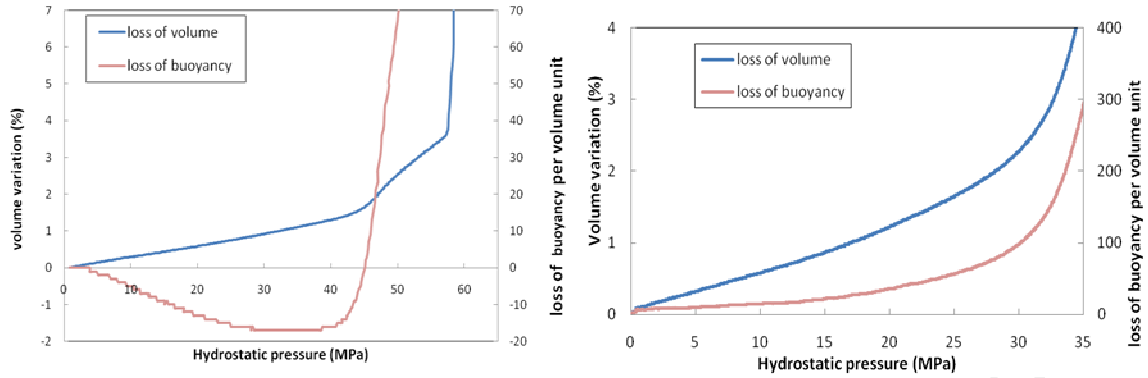

Figure 11. Comparison between loss of volume and loss of buoyancy for GSEP, on the right, and GSPU, on the left, materials under hydrostatic compression test

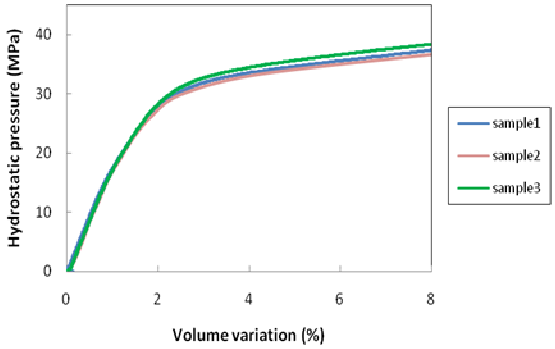

Figure 12. Volume variation of 1dm^3 GSPU samples subjected to hydrostatic pressure

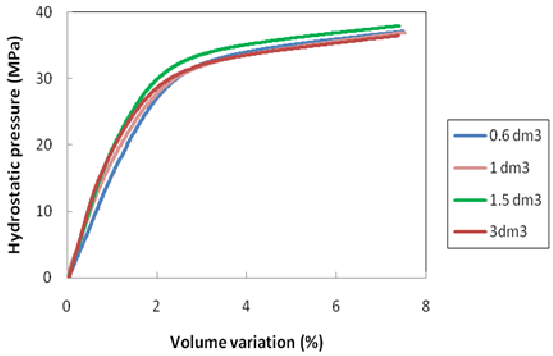

Figure 13. Influence of the volume of sample on hydrostatic compression test results

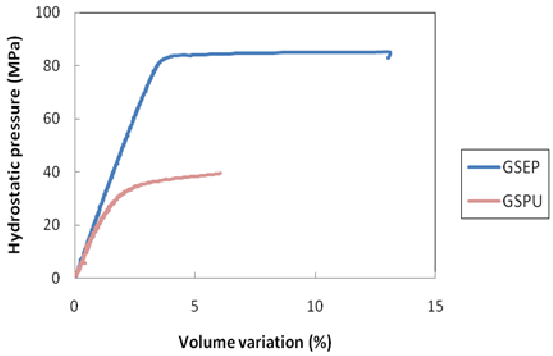

Figure 14. Hydrostatic compression test at 20°C

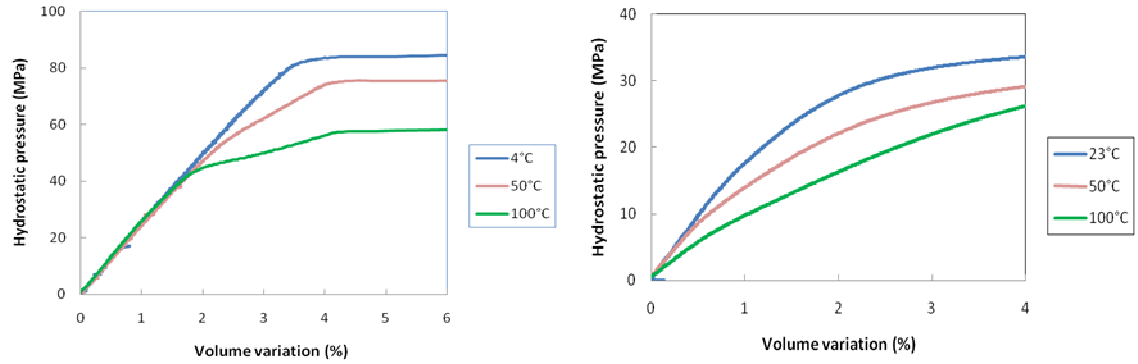

Figure 15. Influence on the temperature for GSEP material, on the left, and GSPU, on the right with hydrostatic compression test